Electrical discharge propagation between GEM foils

A. Utrobicic[c,*], M. Kovacic[b], F. Erhardt[a], M. Jercic[a], D. Karatovic[a], N. Poljak[a], M. Planinic[a]

[a] *Faculty of Science, University of Zagreb, Bijenicka c. 32, 10000 Zagreb, Croatia*
[b] *University of Zagreb, Faculty of Electrical Engineering and Computing, Unska 3, 10000 Zagreb, Croatia*
[c] *European Organization for Nuclear Research (CERN), CH-1211 Geneve 23, Switzerland*

Abstract

This paper presents the studies of fast sequential discharge formations in neighboring Gas Electron Multiplier foils (so called fast discharge propagations). We report on the characteristics of the time delay between the discharges, which has been shown to be of the order of tens of nanoseconds. This time delay decreases both with increasing voltage on the foil where the secondary discharge occurs as well as with decreasing distance between the neighboring foils. Optical measurements of the discharges in two- and three-stage detector setups show that the propagating discharge does not occur directly below the primary discharge, but is displaced from the shortest line between neighboring foils. This observation, together with Scanning Electron Microscope and Energy Dispersive Spectroscopy analyses of the material deposited below the position of the primary discharge provide valuable information on the time evolution of the fast discharge propagation through the detector and its formation mechanism. In the light of these findings, we propose and discuss a new hypothesis for the occurrence of the secondary discharges.

Keywords: GEM, THGEM, discharge propagation

1. Introduction

The Gas Electron Multiplier (GEM) is a gas filled detector which combines a very high rate capability with good spatial resolution and the ability to work in a harsh environment [1, 2]. It works either as a standalone proportional counter or as a cascade of two or more elements. Usually, a multiple GEM layer structure is adopted in order to reach high total gains while operating in safe conditions [3, 4, 5, 6]. The operation of a GEM detector at high rates and high gains may cause an electric discharge inside a GEM foil hole. If a detector is composed of multiple foils, these discharges can trigger a discharge formation in the gap below or above them (so called delayed discharge propagation) or a discharge in the neighboring GEM foil hole placed above or below (so called fast discharge propagation - fast DP). The propagation of discharges from one GEM foil to the next GEM foil or from the last GEM foil to the readout pad can cause damage to the readout electronics due to high energy released in a discharge event. Studies of the delayed DPs and fast DPs between GEMs have been performed alongside GEM detector developments [7, 8, 9, 10, 11]. Recently, the interest in these phenomena has been renewed due to the upgrades of the ALICE and the CMS GEM detector systems [12, 13, 14, 15, 16]. Specifically, studies of the delayed discharge propagation from the last GEM to the readout electrode have been performed both electrically and optically in a setup using a single GEM and a readout anode [17]. Better understanding of these phenomena is necessary to prevent these events and optimize the operational parameters of GEM based detectors.

Earlier electrical measurements of the fast DP between GEMs found that the time delay between the breakdowns was negligible within an accuracy of 10 ns and the occurrence of the DP was independent on the electric field strength between the GEMs [9]. Due to these observations, it was concluded that UV photons created during the primary discharge mediate the fast DP between GEMs. Measurements of the fast DP probability as a function of the receiving GEM voltage for normal and inverted electric field setups between GEMs were performed in a two-stage detector [10]. The fast DP probability had a sharp increase from zero to one after reaching a certain limiting voltage on the GEM to which the discharge propagates (so called receiving GEM). Because fast DPs between GEMs were observed for both the normal and the inverted electrical field setups, it seemed that these phenomena could be explained by the emission and the re-absorption of the photons in the gas or on the metallic electrode. So far, no time delay in fast DPs between GEMs has been observed and no optical measurements have been performed in a setup with multiple GEM foils, enabling one to look at fast GEM to GEM discharges.

2. Experimental setup

The main components of the setup used for the measurements are a single hole thick GEM (THGEM) foil and standard GEM foils placed in a transparent acrylic glass chamber. The THGEM foil is made of a 0.2 mm thick FR4 dielectric material that has a 17.5 μm thick copper layer with an area of 10 x 10 cm^2 on both sides. A single hole, 0.3 mm in diameter, was

*Correspondence to: CERN, 1211 Geneve 23, Switzerland.
Email address: antonija.utrobicic@cern.ch (A. Utrobicic)

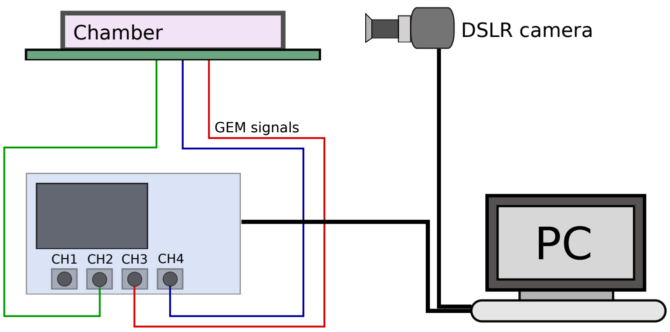

Figure 1: The generalized experimental set-up schematics.

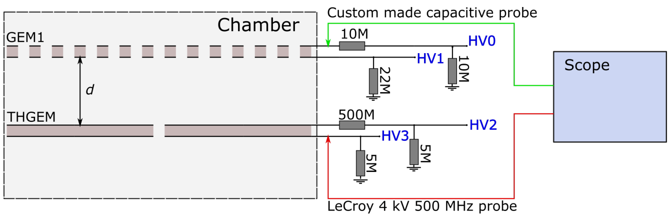

Figure 2: The powering schematics and the chamber layout for studies of the fast DP from single hole THGEM to GEM.

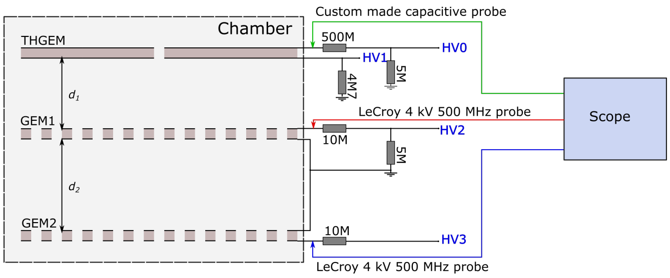

Figure 3: The powering schematics and the chamber layout for studies of fast DPs from GEM1 to GEM2.

drilled through the foil. The standard GEM foils with an area of 10 x 10 cm^2 consist of a dielectric material (polyimide foil 50 μm thick) with a copper layer on both sides (each 5 μm thick) and double conical holes (inner diameter 50 μm and outer diameter 70 μm) extending through the foil with 140 μm pitch. The chamber can be filled with a gas of choice and in these measurements a Ne–CO_2–N_2 (90-10-5) mixture at atmospheric pressure was used. Two types of measurements were made. In the first case, a standard GEM foil was placed above the THGEM so that the fast DP from the THGEM to the GEM could be studied. In the second case, the fast DP from one GEM foil to another was of interest, so two standard GEM foils were placed in a cascade below the THGEM. The single hole THGEM is used to provide control over the position of the primary discharges that were induced by applying an over-voltage to the THGEM electrodes. The single hole THGEM used was made specifically for these and previous measurements described in [17]. A digital single-lens reflex (DSLR) camera was used to record the primary and the delayed discharges. The camera was triggered by an oscilloscope which was set to trigger on the primary discharges. The oscilloscope signals from the THGEM electrode and the GEM electrode(s) were recorded simultaneously with optical measurements by a computer. The generalized schematics of the experimental set-up are shown in figure 1.

The powering schematics used in measurements where a fast DPs from THGEM to GEM were studied are shown in figure 2. Both the THGEM and the GEM foil electrodes were powered through four independent HV channels from an Iseg EHS8080n power supply. A high-value loading resistor of 500 MΩ was used on the THGEM top electrode to reduce the sparking frequency and thus limit the number of sparks recorded by the camera to a single spark. A loading resistor of 10 MΩ was used on the GEM top electrode. Current sinking resistors of 10 MΩ, 22 MΩ, or 5 MΩ were placed between the HV outputs and ground for each channel connected to the THGEM/GEM electrodes. The upper GEM electrode was connected to the oscilloscope through a custom made probe, while the bottom THGEM electrode was connected through a commercial LeCroy HV 4 kV probe.

The powering schematics used in measurements where fast DPs from GEM to GEM were studied are shown in figure 3. Voltages from the THGEM top, GEM1 top and GEM2 bottom electrodes were measured and recorded. The voltage on the top THGEM electrode was measured with the custom made capacitive probe [17], while the voltages from the GEM1 top electrode and the GEM2 bottom electrodes were measured with commercial high voltage LeCroy probes. A high voltage was applied to the THGEM top and bottom electrodes, as well as the GEM1 top and the GEM2 bottom electrodes. The GEM2 top electrode and the GEM1 bottom electrode were grounded.

3. Experimental measurements

3.1. Electrical measurements of the fast discharge propagation from the THGEM to the GEM

Measurements of fast DPs from the THGEM to the GEM were made on a two-stage detector layout, as shown in figure 2. The voltage difference between the GEM top electrode and the ground, and between THGEM bottom electrode and the ground were recorded by an oscilloscope and sent to a computer. A voltage of 900 V was applied across the THGEM electrodes in order to control the appearance of the primary discharge. The voltage on the GEM was gradually increased until a fast DP was observed. The electric field between the THGEM top electrode and the GEM bottom electrode was initially set to zero.

A fast DP from a THGEM to a GEM was observed when a voltage of 425 V was set across the GEM electrodes. Figure 4 (left panel) shows the recorded waveforms for an event where only a primary discharge was observed. The waveforms for an event where both the primary discharge and a fast DP were observed can be seen in figure 4 (right panel) for identical voltage settings. The green signal represents the voltage on the GEM top electrode without the direct current (DC) component, due to the usage of a custom made capacitive probe. The red signal represents the voltage on the THGEM bottom electrode, which is a pure DC signal. The x-axis represents the time, measured in μs, from the moment the primary discharge occurs in the THGEM, and the y-axis represents the voltage from the electrodes in kV.

The discharge formation in the GEM can be seen on the right panel of figure 4 (green waveform) as a rapid increase in the voltage from zero to approximately 450 V. At time t=0 μs large voltage oscillations can be observed due to the primary discharge. To get a better insight into the oscillations after the primary discharge, the recorded voltage waveforms from the GEM top electrode were more closely inspected for an event with the fast DP and an event without it in figure 5.

The measurements on the left panel of figure 5 show that the voltage on the GEM top electrode is similar in trend and amplitude in both cases, namely when a discharge takes place in the GEM or when this does not happen. But, a difference of a few hundred of volts appears approximately 70 ns after the primary discharge in the voltages on the GEM top electrode for an event with a discharge in the GEM, with respect to an event with no discharge in the GEM. This indicates that the primary discharge in the THGEM and the discharge in the GEM did not occur simultaneously, but rather that there is a time delay between them in the range of tens of nanoseconds. This observation indicates that some physical process other than the suggested photo-mechanism [8, 18] could be responsible for the fast DP between the GEMs.

3.2. Measurements of fast DP between two GEMs

In order to test if the same time delay occurs in the case of GEM to GEM discharge propagation we used a three stage detector configuration shown in figure 3. The voltages in the detector were set so that the primary discharge in the THGEM is followed by a fast discharge in GEM1. The voltage across GEM2 electrodes was gradually increased until a discharge on GEM2 was also observed. The transfer field between GEM1 and GEM2 was fixed to zero so that any influence of the charge created during the discharge in GEM1 can be excluded as the source of the discharge formation in GEM2. The transfer gap length between the THGEM and GEM1 was set to 2 mm and the transfer gap length between GEM1 and GEM 2 was set either to 2 mm or to 6 mm. The voltages applied in the setup for the performed measurements are shown in table 1.

Table 1: The set electrode voltages for GEM to GEM fast DP studies with 2 mm and 6 mm transfer gap lengths. The GEM1 bottom and the GEM2 top electrodes are set to GND.

$THGEM_{top}$	$THGEM_{bott}$	$GEM1_{top}$	$GEM2_{bott}$ $d_{tr} = 2\ mm$	$GEM2_{bott}$ $d_{tr} = 6\ mm$
-1550 V	-550 V	-458 V	-416 V	-458 V
-1550 V	-550 V	-458 V	-425 V	-467 V
-1550 V	-550 V	-458 V	-441 V	-475 V
-1550 V	-550 V	-458 V	-458 V	

When the voltage between the GEM2 electrodes was set to 416 V (458 V), a fast discharge propagation to GEM2 was observed for a 2 (6) mm transfer gap. The recorded voltages on the TH(GEM) electrodes are shown in figure 6 for the 2 mm transfer gap. The left panel shows a primary discharge in the THGEM (green signal) at t=0 μs, followed by a discharge in GEM1 (red signal) 10 ns later. The recorded voltage from the GEM2 bottom electrode (blue) shows no discharge in GEM2 during this event. For identical voltage settings in the setup, the right panel of figure 6 shows an event where a discharge in GEM2 is observed approximately 70 (60) ns after the primary discharge in the THGEM (GEM1).

We observed that the time delay between the discharges in the GEM foils decreases with increasing GEM2 voltages, as shown in figure 7 (left panel). Conversely, the time delay increases when increasing the transfer gap length between the GEM foils, also shown in figure 7 (left panel).

The probability of the fast discharge propagation was calculated as the ratio of the observed discharges in GEM2 and the total number of primary discharges. A binomial error was employed to determine the uncertainty of the fast discharge propagation probability. Measurements show that the fast discharge propagation probability strongly depends on the receiving GEM (GEM2) voltage, as observed in earlier measurements [10]. The probability has a sharp increase from zero to one at a certain GEM2 voltage as shown in figure 7 (right panel).

The measurements performed with a fixed zero transfer field topology show that the discharge propagates between adjacent GEM foils in a not negligible time delay, which increases with increasing transfer gap length. These results may indicate that some physics which does not include emitted photons is responsible for the fast DP between GEMs. The performed measurements motivated a more detailed research of the fast DP by using a quartz glass plate and performing both lateral and top side optical recordings.

4. Measurements with quartz glass

Additional measurements were made by placing a transparent piece of 0.2 mm thick quartz glass above the THGEM hole in order to create a UV transparent mechanical barrier. The purpose of this barrier was to block any material possibly ejected during the primary discharge, but to allow UV light created during the primary discharge to pass through it.

The topology of the setup can be seen in figure 8. In these measurements, the transfer field length was set to 2 mm and the electrode voltages were set to -100 V, -1000 V, -1100 V, and -1500 V to -1600 V for the THGEM bottom, THGEM top, GEM bottom and GEM top electrodes, respectively. The voltage applied across the GEM foil electrodes was increased in steps of 20 V from 400 V up to 500 V.

If fast DP occurs due to photons, a transparent piece of glass should not prevent it from happening. In our measurements, we found that the secondary discharge never appears if the piece of glass is placed above the hole facing the adjacent GEM foil, even if the voltage on GEM foil is increased up to 500 V. This, alongside our previous measurements led us to believe that a mechanism different from UV propagation causes the fast DP.

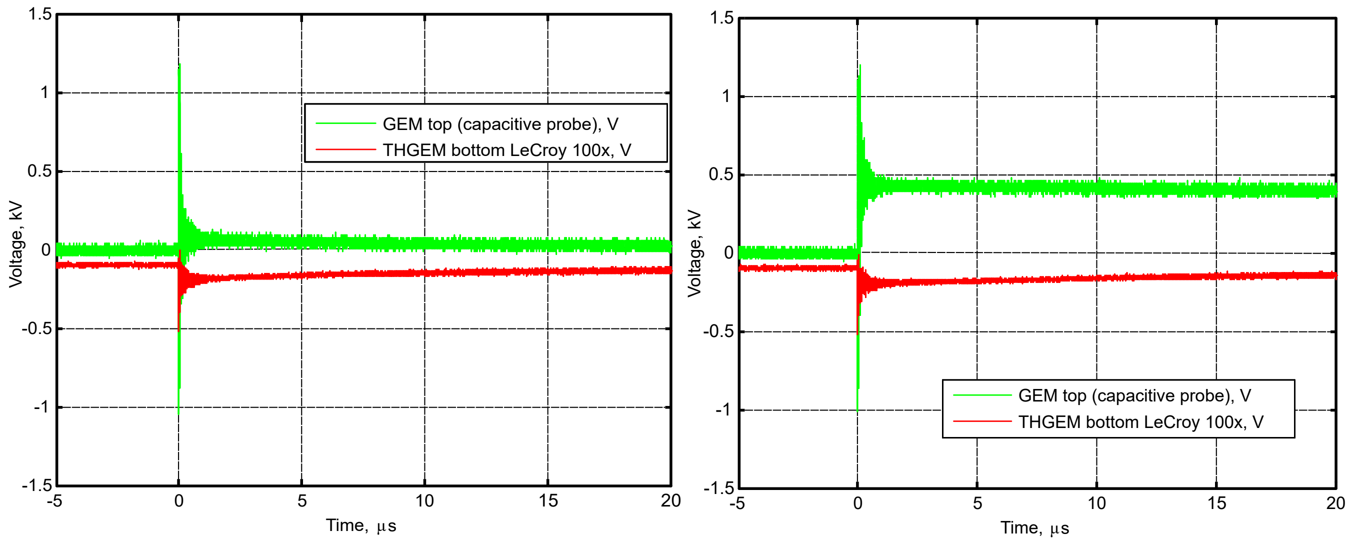

Figure 4: Recorded waveforms for an event with a primary discharge in the THGEM and no discharge in the GEM (left panel) and an event with a primary discharge followed by a discharge in the GEM (right panel). The electrode voltages before the discharges were -100 V, -1000 V, -1000 V and -1425 V on the THGEM bottom, THGEM top, GEM bottom and GEM top electrode, respectively. (For interpretation of the references to color in this figure legend, the reader is referred to the web version of this article.)

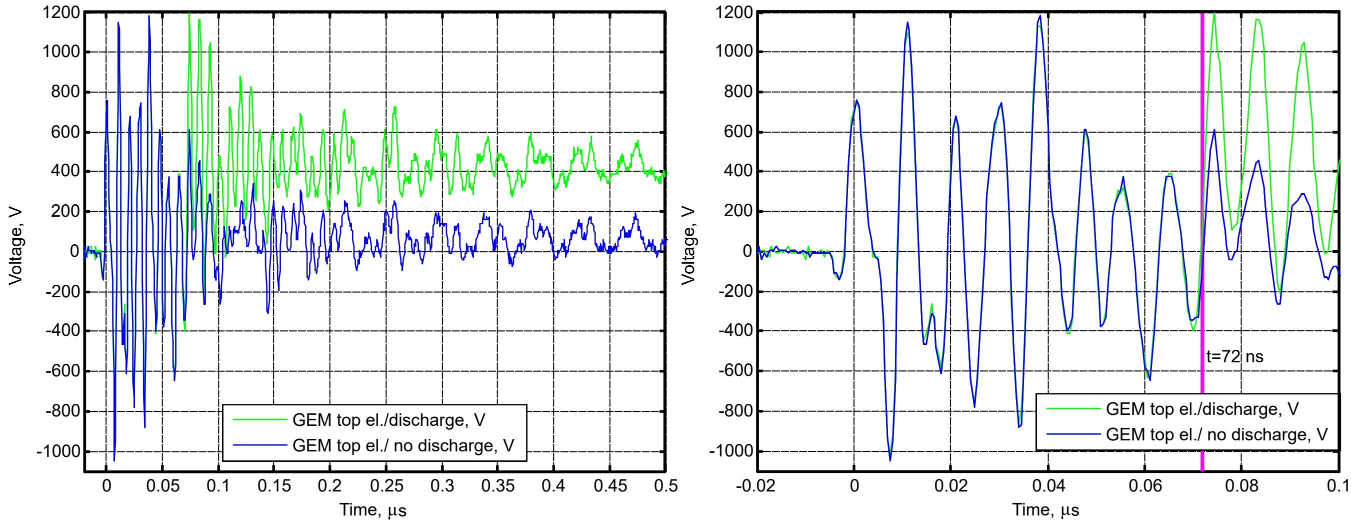

Figure 5: Comparison of the voltages from the GEM top electrode for an event with only a primary discharge in the THGEM (blue waveform) and an event with a primary discharge in the THGEM followed by a discharge in the GEM (green waveform). The left panel shows the waveforms during the 500 ns after the primary discharge, while the right panel shows the waveforms during the 100 ns after the primary discharge. (For interpretation of the references to color in this figure legend, the reader is referred to the web version of this article.)

5. Optical measurements

To gain further insight into the discharge mechanism, we performed additional measurements with synchronised electrical and DSLR camera measurements. Optical recordings of the fast DP were obtained either laterally or from the top of the setup.

Recordings from a configuration in which a GEM foil was placed 2 mm above the single hole THGEM are shown in figure 9. The top panel shows the top view (left panel) and the lateral view (right panel) of a discharge propagation. It can be seen that the discharge in the GEM foil is spatially displaced from the position of the primary discharge with respect to the shortest line between the foils. The same type of spatial displacement between discharges can be seen in the optical recordings for a three stage detector configuration with a single THGEM foil and two GEM foils beneath it, as shown in the bottom panel. In this case, after inducing the primary discharge in the THGEM foil, we observed a spatially displaced discharge in the next foil, followed by a displaced discharge in the final foil.

It is interesting to note that there is no immediate reason as to why the discharges should be displaced spatially. This could indicate that some kind of an anisotropy is present in the

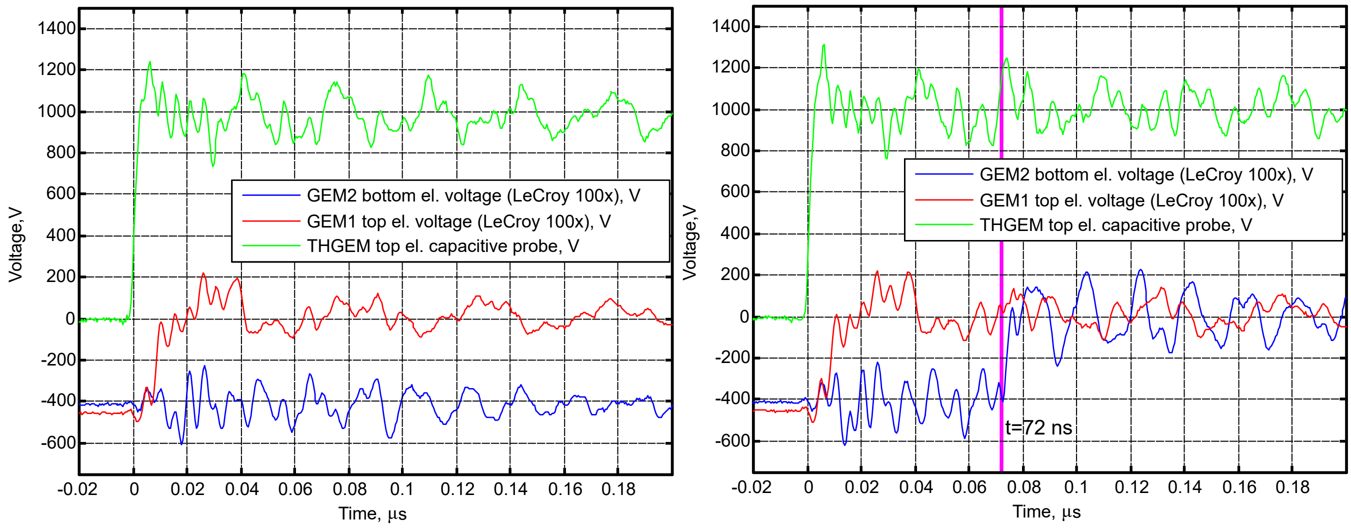

Figure 6: Recorded waveforms from the THGEM top (green), GEM1 top (red) and GEM2 bottom (blue) electrodes for an event with discharges in the THGEM and GEM1, but not in GEM2 (left panel) and an event with discharges in all three GEMs (right panel). (For interpretation of the references to color in this figure legend, the reader is referred to the web version of this article.)

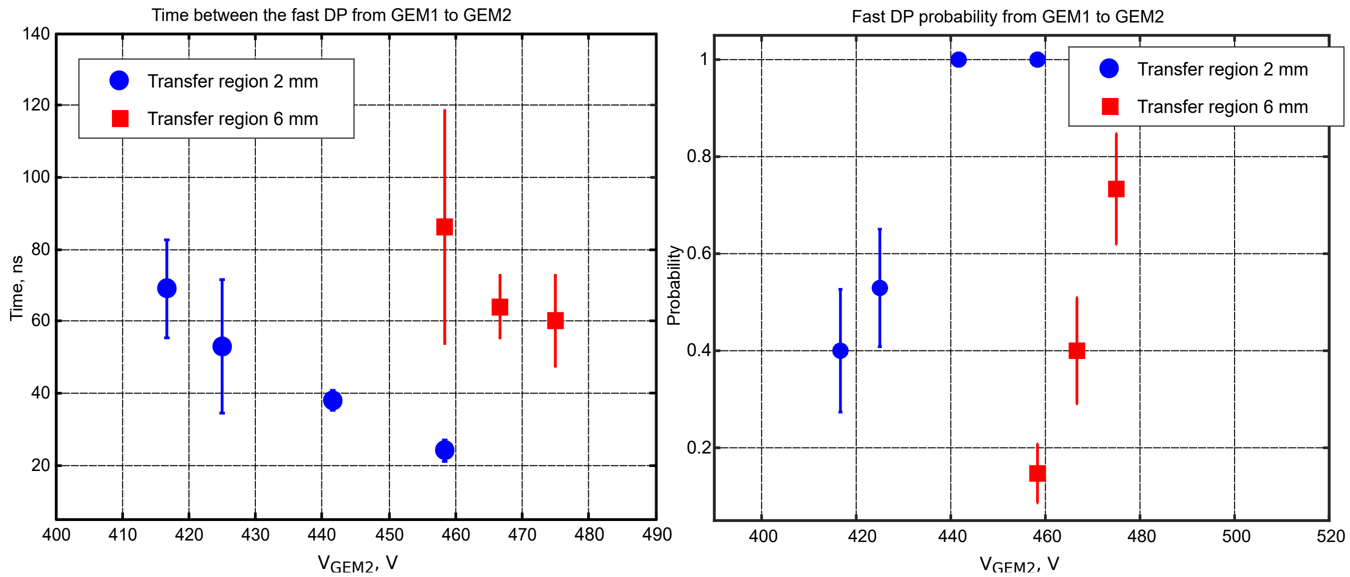

Figure 7: Time delay between the discharge in GEM1 and the discharge in GEM2 for 2 mm (circles) and 6 mm (squares) transfer gap lengths is shown on the left panel. The fast discharge propagation probability for 2 mm (circles) and 6 mm (squares) transfer gap lengths is shown on the right panel.

system. This fact, along with the already mentioned result that the time delay between the discharges increases with increasing distance between the GEMs led us to formulate a new hypothesis.

6. The plasma mechanism and the SEM analysis

Motivated by the collected evidence, we were led to believe that the plasma created during the primary discharge causes the surrounding material to melt and detach from the (TH)GEM structure. The material within the hole and surrounding it can then be ejected above and below the hole during the primary discharge due to the high pressure inside the hole. Specifically, molten copper is torn from the (TH)GEM hole rim, which forms a conical shape. When the hot conductive copper gets in close vicinity of the neighbouring GEM foil hole, it can significantly alter the local electrical field and cause a breakdown.

To verify or disprove our hypothesis, we induced a large number of primary discharges in a single hole THGEM and wanted to see if there is any material deposition on the neighboring structure. The setup used for these measurements is schematically shown in figure 10. This setup was also connected to a camera to make sure that fast DPs are caused in the top GEM foil. The experimental setup and an optical recording

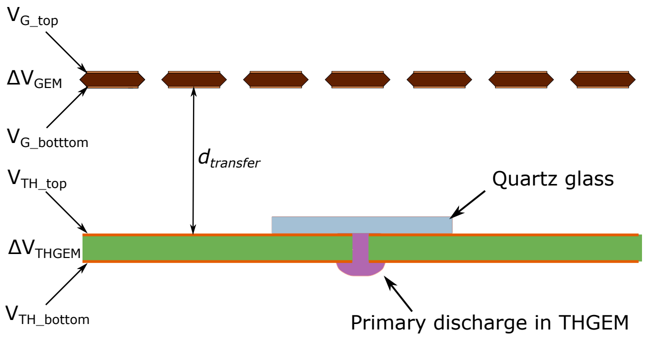

Figure 8: The cross section of the setup used for the tests with the quartz glass.

of some of these double discharges are shown in figures 11 and 12.

To perform an elemental analysis using a Scanning Electron Microscope (SEM) and Energy Dispersive Spectroscopy (EDS), a plate was needed to collect material on. The collection plate was made of pure silicon. A large number of discharges (> 1000) was then induced in the THGEM foil. The plate containing the accumulated material was removed from the setup and taken to be analysed. An image from the analysis with a 10x magnification is presented in figure 13. An accumulation of material can be clearly seen as a different hue, located near the point that was on the axis of the original THGEM foil hole, denoted as "primary location" in further text.

Zooming in closer near the primary location, one can notice both irregularly shaped and nearly spherical structures. The sizes of these structures are comparable to each other and of the order of a few micrometers. Both of these types of structures can be seen magnified in figure 14.

The EDS analysis revealed the chemical composition of the material in these structures. Probing a few of them, we noticed a large difference in their compositions. Whereas the irregular structures are composed mainly of silicon and oxygen, accounting for over 90% of their weight, the regular, spherically shaped structures are composed mostly of copper and bromine, with some inclusions of carbon and silicon. The chemical composition of a spherical particle (figure 15) located 1 mm from the primary location is given in table 2. To put that in contrast, the chemical composition of one of the irregular structures scattered around the primary location (figure 15, bottom right panel) is given in table 3.

Additional analysis of other spherical and irregular structures confirms the already found compositions: the spherical structures consist mostly of copper, while the irregular ones are mostly silicon. A larger concentration of the irregularly shaped structures can be found directly below the primary discharge position, while already 1 mm away from it, their concentration decreases rapidly. The inverse holds true for the spherical structures. From this, we conclude that the irregular structures are parts of the ejected GEM foil interior (hole walls) and the spherical structures are droplets of copper formed by the plasma heating of the GEM hole copper edge that is removed and found after the material was ejected.

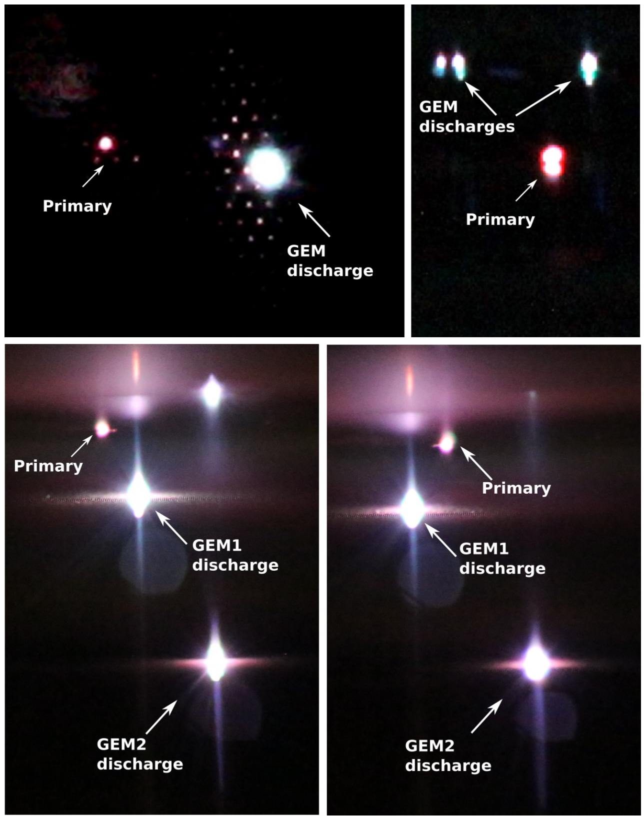

Figure 9: An example of the top view (top panel, left) and a lateral view (top panel, right) of a discharge propagation in a two stage detector configuration. The bottom panel shows optical recordings from a three stage detector configuration as described in section 3. The discharges in adjacent foils are clearly spatially displaced with respect to the shortest line between the foils.

Table 2: The chemical composition of a spherical particle shown on the left panel of figure 15.

element	weight %	atomic %
C	2.47	11.88
O	1.13	4.07
Si	2.59	5.33
Cu	58.75	53.39
Br	35.06	25.34

7. Discussion and conclusion

We performed detailed electrical and optical measurements of fast GEM to GEM discharge propagations. Electrical measurements of the GEM electrode voltage provided an insight

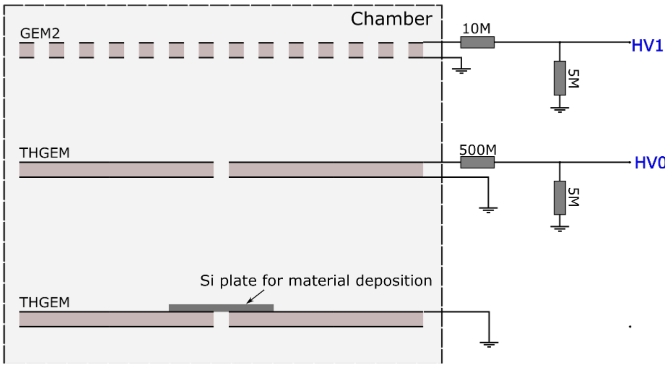

Figure 10: The schematics of the setup used to collect the material from the primary THGEM discharges. In this setup, the THGEM discharges are caused by an overvoltage. The discharges induce secondary discharges in the GEM foil above them and deposit material on the Si plate placed on the foil below.

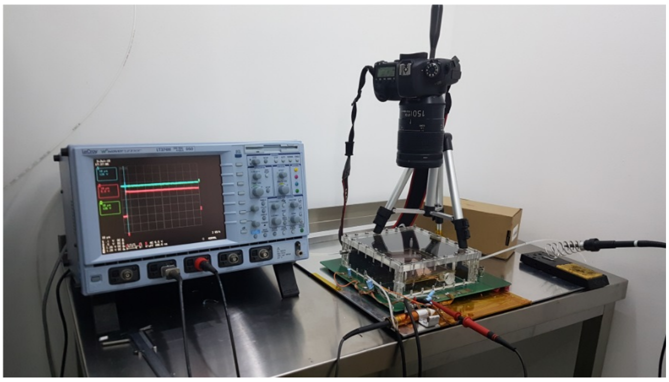

Figure 11: The experimental setup used to collect the material from the primary GEM discharges. The DSLR was in this case placed on top of the setup, providing images which show a clear spatial displacement of the primary and the secondary discharges.

Table 3: The chemical composition of an irregularly shaped structure shown on the bottom right panel of figure 15.

element	weight %	atomic %
C	2.96	6.51
O	5.94	9.81
Si	86.92	81.74
Ca	1.18	0.78
Cu	2.02	0.84
Br	0.97	0.32

into the temporal evolution of the DP propagation through the detector. Thanks to the specially developed setup with a minimal inductance between the point of measurement and the GEM electrode it was possible to reduce the noise caused by the primary discharge and distinguish it from the propagating discharge. This enabled the observation of the time delay between the primary discharge in the THGEM and the secondary discharge in the GEM foil. The observed time delay is in a range of tens of nanoseconds and it increases either when reducing

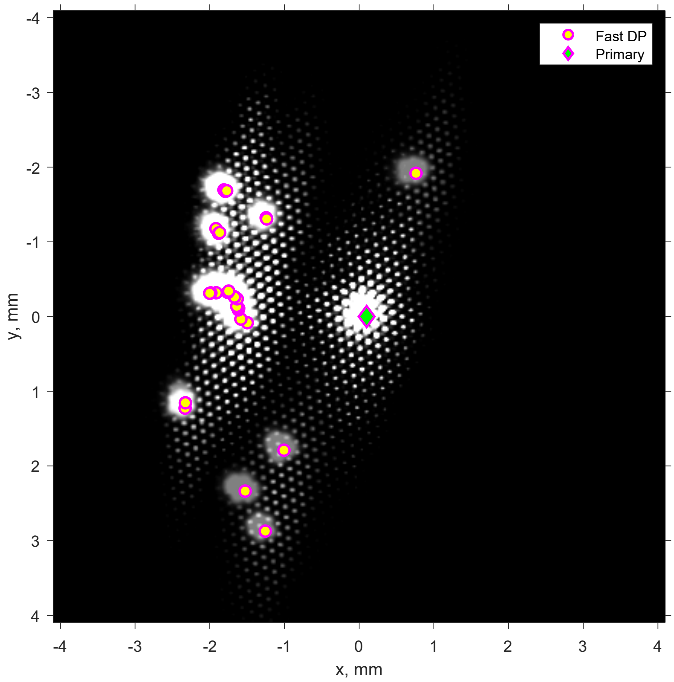

Figure 12: Top view of 30 primary and secondary discharges stacked in a single image. Each discharge centre is obtained from one of the frames using the center of mass method.

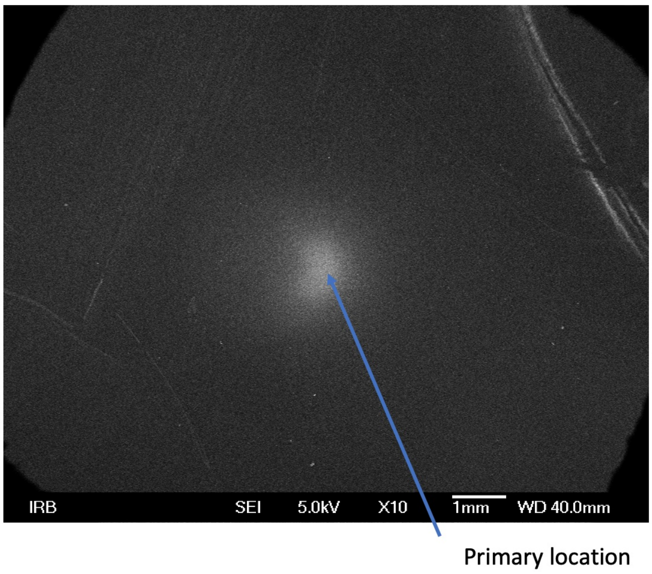

Figure 13: A SEM image of the foil containing the material ejected from the THGEM discharges. The blue arrow points to the point that was located on the axis of the original THGEM foil hole.

the voltage of the receiving GEM or when increasing the distance between the GEM foils. This indicated that there might a mechanism that is not photon induced and is responsible for the fast DPs between the GEMs.

The optical recordings of the discharges show that the primary discharge and the propagating discharge are spatially dis-

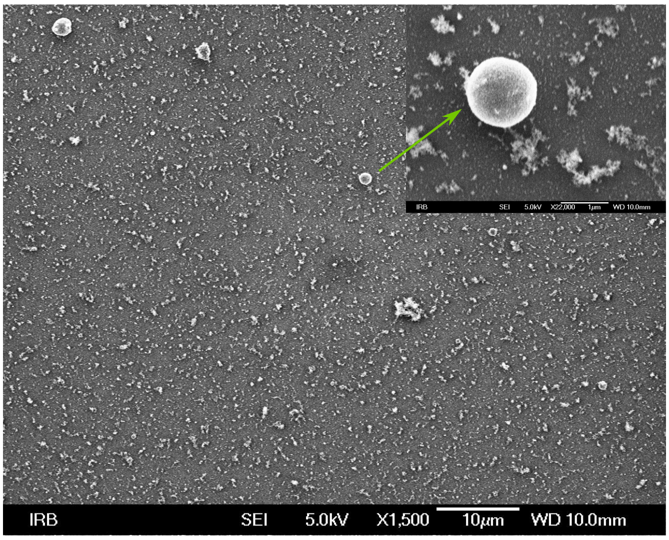

Figure 14: A closer view of the material near the primary location reveals two types of structures: spherically shaped particles and irregularly shaped material. The inset on the right shows a magnified view of a spherically shaped particle.

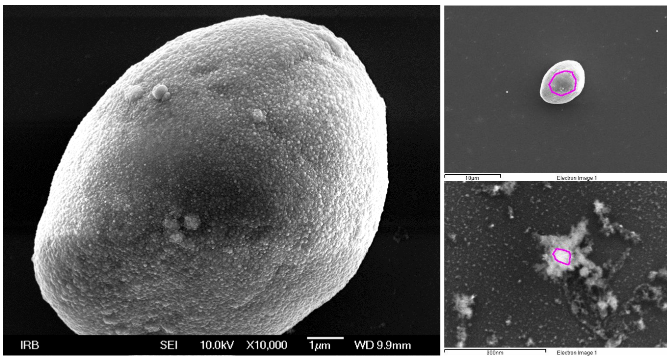

Figure 15: The left panel shows a close-up view of one of the spherical particles found 1 mm from the primary location. The right panel (top) shows the same particle on a larger scale. The right panel (bottom) shows a magnified view of an irregularly shaped deposit near the primary location.

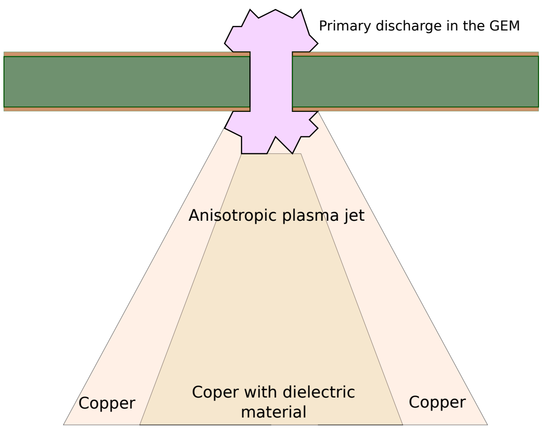

Figure 16: Sketch of the proposed mechanism for the explanation of the fast DPs between GEMs.

placed. An interesting observation was that the DP usually occurs 1-2 mm away from the primary, but not directly below it, figure 12.

This motivated a proposal of a new hypothesis for the occurrence of fast DPs between neighboring GEM foils. The primary discharge creates a high temperature plasma within a GEM hole and its surrounding area. The dielectric material within the hole and the copper surrounding the hole melt and deteriorate. Due to the high pressure in the hole, material is ejected in the form of a jet. The outer part of the jet should contain most of the copper from the rim, while the inner part should contain the dielectric material, mixed with some copper, as sketched in figure 16. If the conductive heated material gets in the vicinity of the adjacent GEM foil hole, it can significantly alter the local electric field and cause a breakdown. This can explain the occurrence of the spatially displaced fast DP with respect to the preceding discharge position.

The observed increase in the discharge propagation onset voltage at a larger transfer gap (Figure 7) was not analyzed within this paper. The authors are of the opinion that it can be caused by the diffusion of the ejected material and the reduction of its temperature. Further studies and development of a new experimental method are required to get more insights into this observation.

Initial SEM and EDS analyses of the material deposited below the primary discharge show promising results. Material deposition was observed in a small area below the primary discharge. Based on the morphology of the observed particles in the deposit there were two types of structures identified: irregularly shaped and nearly spherically shaped. The spherical structures consist mostly of copper, while the irregular ones are mostly silicon and elements that can be found in the FR4 material. These results confirm our hypothesis that the conductive material detached from the hole rim during the primary discharge is responsible for fast DPs in neighboring GEM foils.

Acknowledgements

This work has been fully supported by the Croatian Science Foundation project IP-2018-01-4108. We want to thank to the RD51 collaboration members for useful discussions during this research.

References

[1] F. Sauli, Nucl. Instr. and Meth. A 386 (2) (1997) 531–534. doi:10.1016/S0168-9002(96)01172-2.
[2] F. Sauli, The gas electron multiplier (gem): Operating principles and applications, Nucl. Instr. and Meth. A 805 (2016) 2–24. doi:10.1016/j.nima.2015.07.060.
[3] B. Ketzer, Q. Weitzel, S. Paul, F. Sauli, L. Ropelewski, Nucl. Instr. and Meth. A 535 (1) (2004) 314–318. doi:10.1016/j.nima.2004.07.146.
[4] M. Bagliesi, M. Berretti, E. Brucken, R. Cecchi, E. David, F. Garcia, V. Greco, J. Heino, T. Hilden, K. Kurvinen, et al., Nucl. Instr. and Meth. A 617 (1) (2010) 134–137. doi:10.1016/j.nima.2009.07.006.

[5] H. Appelshaeuser, C. Lippmann, P. Christiansen, C. Garabatos, N. Smirnov, J. Harris, A. Oskarsson, M. Ball, J. Wiechula, T. Gunji, et al., Technical design report of the alice tpc upgrade, Tech. rep. (2013).

[6] D. Abbaneo, C. Armagnaud, M. Abbrescia, P. Aspell, S. Bally, Y. Ban, L. Benussi, U. Berzano, S. Bianco, J. Bos, et al., Nucl. Instr. and Meth. A 718 (2013) 383–386. doi:10.1016/j.nima.2012.10.058.

[7] T. Zeuner, H.-B. I. T. Collaboration, et al., Nucl. Instr. and Meth. A 446 (1-2) (2000) 324–330. doi:10.1016/S0168-9002(00)00042-5.

[8] C. Iacobaeus, A. Brahme, M. Danielsson, P. Fonte, J. Ostling, V. Peskov, M. Wallmark, IEEE Transactions on Nuclear Science 48 (4) (2001) 1496–1502. doi:10.1109/23.958386.

[9] M. Wallmark, A. Brahme, M. Danielsson, P. Fonte, C. Iacobaeus, V. Peskov, J. Östling, Nucl. Instr. and Meth. A 471 (1-2) (2001) 151–155. doi:10.1016/S0168-9002(01)00980-9.

[10] S. Bachmann, A. Bressan, M. Capeáns, M. Deutel, S. Kappler, B. Ketzer, A. Polouektov, L. Ropelewski, F. Sauli, E. Schulte, et al., Nucl. Instr. and Meth. A 479 (2-3) (2002) 294–308. doi:10.1016/S0168-9002(01)00931-7.

[11] V. Peskov, P. Fonte, Research on discharges in micropattern and small gap gaseous detectors, arXiv preprint arXiv:0911.0463.

[12] F. Ivone, Discharge mitigation strategies for ge11 detectors in the cms experiment, Ph.D. thesis, Universita e INFN, Bari (IT).

[13] J. A. Merlin, Discharge effect in gems status and update, Talk at the GDD meeting, https://indico.cern.ch/event/702782/ (2018).

[14] J. A. Merlin, Study of discharges and their effects in gem detectors, Talk at the MPGD 2019 conference, https://indico.cern.ch/event/757322/contributions/3396501/ (2019).

[15] A. Deisting, C. Garabatos, Discharge and stability studies for the new readout chambers of the upgraded alice tpc, Journal of Instrumentation 12 (05) (2017) C05017.

[16] A. Deisting, C. Garabatos, P. Gasik, D. Baitinger, A. Berdnikova, M. Blidaru, A. Datz, F. Dufter, S. Hassan, T. Klemenz, et al., Nucl. Instr. and Meth. A 937 (2019) 168–180.

[17] A. Utrobicic, M. Kovacic, F. Erhardt, M. Jercic, N. Poljak, M. Planinic, Nucl. Instr. and Meth. A 940 (2019) 262–273. doi:10.1016/j.nima.2019.06.018.

[18] J. Ostling, M. Wallmark, A. Brahme, M. Danielsson, C. Jacobaeus, P. Fonte, V. Peskov, Prog. Biomed. Opt. Imaging 3977 (2000) 84.